

# DPIV Measurements of Dynamic Flow Patterns in a Realistic Model of the Lung Airways Down to the 6th Generation

**Katrin Adler<sup>1</sup>, Wolfgang Schröder<sup>2</sup>, Christoph Brücker<sup>3</sup>**

1, 3: Institut für Mechanik und Fluidodynamik, TU-Bergakademie Freiberg, 09596 Freiberg, Germany,  
Katrin.Adler@imfd.tu-freiberg.de, Bruecker@imfd.tu-freiberg.de

2: Aerodynamisches Institut der RWTH Aachen, D-52062 Aachen, Germany, office@aia.rwth-aachen.de

---

**Abstract** The objective of the study is a more detailed analysis of lung ventilation under normal breathing conditions and for artificial, respirator-assisted ventilation. Therefore a realistic 3D model of the lung down to the 6<sup>th</sup> generation was generated to investigate the oscillatory flow through the branching network by DPIV. A transparent model made of silicone is used in combination with a refractive index matching fluid (water/glycerin). The Measurements were carried out using hydrogen bubbles as tracer particles. The mass flow rate and the frequency were adapted to the characteristic flow parameters of the air flow in the human lung keeping the Reynolds- and Womersley-number constant. A first comparison of the results for the inspiration and expiration phase demonstrates the different nature of the flow. During inspiration one can see larger flow separation regions at the outer walls of the bifurcating channels which sometimes extend downstream to the next bifurcation. In contrast, the flow at expiration does not separate at all and shows the typical jet-like profile at the exit of the trachea. The complete cycle of inspiration and expiration suggests that due to the transformation of the velocity profiles and the generated separation regions a net mass flow is created into the model along the centerline and the inner walls of the bifurcations. This is compensated with a net mass outflow to the trachea along the outer walls of the branches along the separation regions which are washed upstream during expiration. At higher breathing frequencies this effect is enhanced which may help to remove deposited particles in the lung network.

---

## 1. Introduction

The lung has often been treated as monoalveolar lung with a quasi-linear behavior. When ventilated, this assumption can lead to an over-expansion of the lung areas and cause lung injuries (Trembley & Slubky 1998). A reason for those injuries can be a bronchus, blocked by secretion or a bad distribution of air caused by wrong ventilation. This is mostly observed for young children who can suffer from an acute respiratory distress syndrome. A result is a collapse of the lung and an over expansion of the alveoli, respectively. This effect is even enhanced by artificial ventilation. The dynamic of these over-expansions has not been investigated so far. Possibilities for a therapy are high frequency ventilation (Rettwiz-Volk et. al. 1993) or independent lung ventilation (Marraro 1992) whereat each lobe of the lung is ventilated separately. Fredberg et. al. (1984) have shown that the local distribution of air and the change of the pressure in the alveoli with time during ventilation can be influenced with a ventilation frequency close to the resonant frequency. They speculated that by variation of the frequency and the pressure distribution, the ventilation of different areas of the lung can be controlled. The aim of the work is the detailed investigation of mass flow distribution in a realistic lung model. Starting from that different protective ventilation patterns are performed and methods are tested in order to manipulate the mainflow direction into selected branches of the lung in order to yield selective lung ventilation.

In the present paper we investigate the different in- and outflow patterns for different flow conditions at an in-vitro model of the human lung. Since for the upper airways the terms of inertia prevail the friction terms the flow through the first branches of the lung is characterized by separation regions, secondary flows and fluctuating free cross sections (Brücker et. al. 2003). The oscillating flow also causes mass exchanges, known as Pendelluft between adjacent branches (Ulmann et. al. 1988).

## 2. Experimental methods

### 2.1 Experimental model

A realistic lung geometry of the upper 6 bifurcation generations was generated as a CAD model and has been casted in a fully transparent silicone block in order to allow optical access. The geometry of the airways is based on two different data sets. The trachea and the subsequent bifurcation, i.e. generation 0 and 1 were designed based on Horsfield (1971) data in order to achieve a realistic lung design. The radius of the curvature as well as the transition zone between the parent and daughter branches were based on Horsfield data, too. He described that the transition zone is subdivided into an elliptical and a carinal region. In the elliptical region of the transition zone, the cross-section changes its shape from circular to elliptical, keeping the cross-section area constant. Within the carinal region the cross section becomes more flattened, so that its smaller axis approximates to the diameter of the daughter branches. Finally this section divides into two circular branches. Lengths and diameters of the generations 2 to 6 were designed following the rules of Weibel (1963) for an ideal bifurcation of the lung. The complete lung model is shown in figure 1.

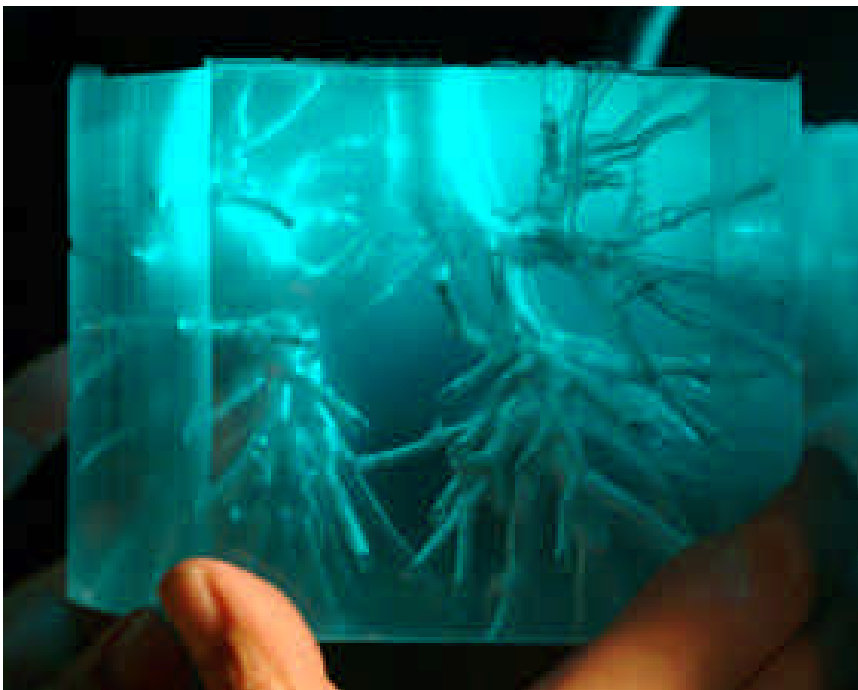


**Fig. 1** Silicone model of the human lung

## 2.2 Experimental set-up

The silicone block with the internal hollow branches of the bronchial tree was placed within a flow loop as shown in figure 2 (*left*). Alternatively a pulsating flow (Fig. 2 *right*) was generated using a linear actuator (MOOG, G400 Series).

The refractive index of the silicone model is  $n = 1.4095$  and can be matched with a water/glycerin mixture with a ratio of 45:55 (volume ratio water:glycerin) in order to prevent optical distortions during the view into the inner part of the model. Since a liquid is used as working fluid the mass flow rate and the frequency during the oscillation had to be adapted according to normal breathing conditions keeping the Reynolds-Number, the Strouhal-Number and the Womersley-Number, respectively, constant. In the case of the oscillating flow the Reynolds-number is defined with the breathing frequency and the tidal volume  $\Delta V$  according to equation 1

$$Re = \frac{\Delta V \cdot f}{u \cdot d} \quad (1)$$

Then the Strouhal-number can be calculated by

$$Sr = \frac{d^2 \cdot f}{u \cdot Re} \quad (2)$$

And Womersley-number is defined by

$$Wo = R \sqrt{\frac{w}{u}} \quad (3)$$

Flow visualization and quantitative flow measurements were done using hydrogen bubbles as tracer particles which were recorded by a CCD camera. (PCO.1600, 1600x1200 pixels resolution, 15 fps at full resolution, 2GB camRAM). First results were obtained for stationary inflow conditions in the trachea.

The experiments with stationary inspiration flow were carried out at a Reynolds-number of  $Re = 1000$  defined with the inlet tube diameter ( $\varnothing = 2$  cm) which is approximately the diameter of the trachea and the mean bulk flow velocity for peak inspiration flow rate under normal breathing conditions at rest with a respiratory volume of  $\Delta V = 0.5l$ . In addition to the stationary inflow conditions the measurements were carried out also for pulsating flow conditions at a physiological Strouhal-number of  $Sr = 0.01$  and a Womersley-Number of  $Wo = 3.24$  for breathing at rest conditions. To study the effect of clinical high-frequency ventilation support devices, higher frequencies were simulated, too. For all the above given cases, DPIV-measurements were taken in different light-sheet positions and for several regions of the branching network. The laser used for the measurements is a 120mJ Nd:YAG double pulse laser. The time delay between two subsequent pulses was 400 $\mu$ s. During stationary flow conditions pictures were taken at a frequency of 5Hz.

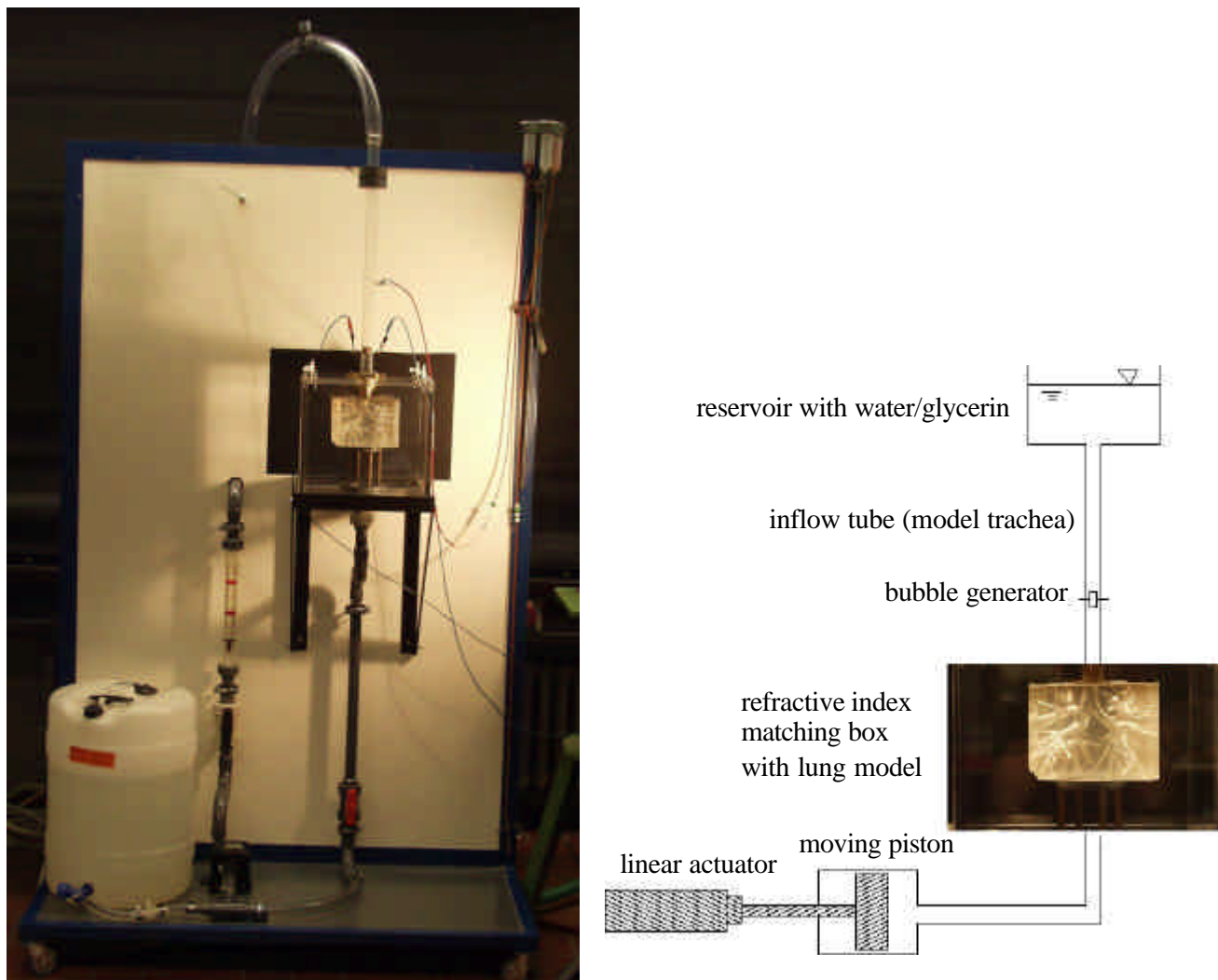


**Fig. 2 a** Test stand for stationary flow conditions (*left*), schematic set-up for pulsatile flow conditions (*right*)

### 3. Results and Discussion

The cross correlation of the pictures was performed within an interrogation size of  $32 \times 32$ . This window size yields finally to a grid spacing of  $16 \times 16$  pixels. In order to keep time and effort of the cross correlation at a minimum level parts of the airways which are not within the illuminated light sheet planes but still lightened from background reflections were masked out before image processing.

For the stationary inspiration flow, PIV-measurements were performed at several parallel planes within the lung model. Altogether these were 16 planes with a spacing of 5mm between each other. In addition measurements with an enlarged view at selected generations have been performed. These generations are the first, second, third and fourth. The results shown here focus on the center plane which is aligned with the flow axis in the trachea and the plane of the first bifurcation.

For the oscillatory flow conditions, the results at different frequencies were compared to each other. Measurements were also carried out with higher magnification at the upper generations. Figure 3) shows the sections of the lung which were investigated using an enlarged view. This figure also illustrates the effect of scattered light due to the hydrogen bubbles.

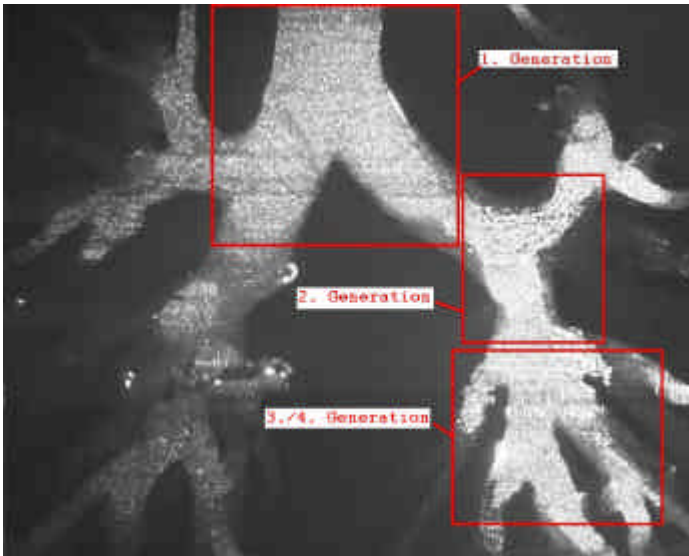


**Fig. 3** Illuminated lung with tracer bubbles and selected sections for the flow analysis

#### 4.1 Stationary flow conditions

Figure shows the results for the flow field in the centerplane by means of the velocity field and the vorticity distribution, respectively for the first four generations. The enlarged sections were arranged together in one picture. The red and blue colours in figure 4 *left* highlight the regions of maximum and minimum vorticity levels (positive and negative rotation) normal to the light-sheet plane and give an impression of the shear distribution within the daughter branches. The interface between red and blue fields indicates the main flow passage along the bifurcation network representing the region of minimum amount of viscous shear  $|w_z|_{\min}$ . It can be seen, that the main flow always follows the path of the minimum change of flow direction. This result lets recognize a preferential pathway through the network with alternated flow separations from the parent to the daughter branch as indicated by the black arrows in figure 4 *left*. This main flow direction can also be seen in figure 4 *right* by the increased magnitude of the velocity vectors along the main path.

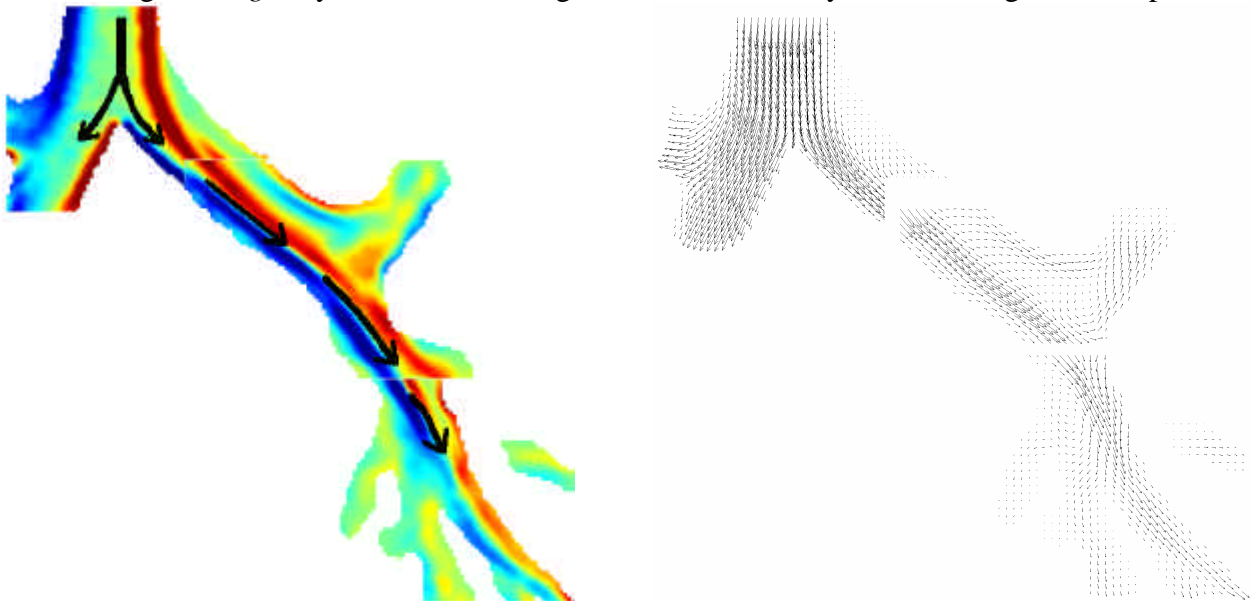


**Fig. 4** steady flow, corresponding to peak inspiration with  $Re = 1000$ , vorticity distribution (*left*) showing the main flow passage in the lung airways, red colours - positive rotation, blue colours – negative rotation, velocity vectors of the 1<sup>st</sup> to 4<sup>th</sup> generation (*right*)

A study of the fluctuating velocities was performed for the stationary inflow conditions. Figure 5 shows the standard deviation of the velocity field, normalized with the magnitude of the mean velocity. The maximum deviation was 0.3 and is marked by the red isolines in figure 5. The minimum standard deviation is 0.05 and represented by the dark blue lines. The isolines of the standard deviation are superposed with the velocity field (Fig. 5 *right*) in order to get an impression of the location of the maximum standard deviation within the bifurcations.

In the trachea and the first generation these fluctuations occur mainly near the tube walls and in the flow separation regions. The main flow path is almost free of oscillations although it is located in the region of the maximum velocity. Further downstream the fluctuations are shifted to the location of the main flow passage (Fig. 5 *right*). This fluctuation field lets recognize that the lung geometry is characterized by high fluctuations although stationary flow conditions were used. The largest fluctuations occur in the areas of high vorticity.

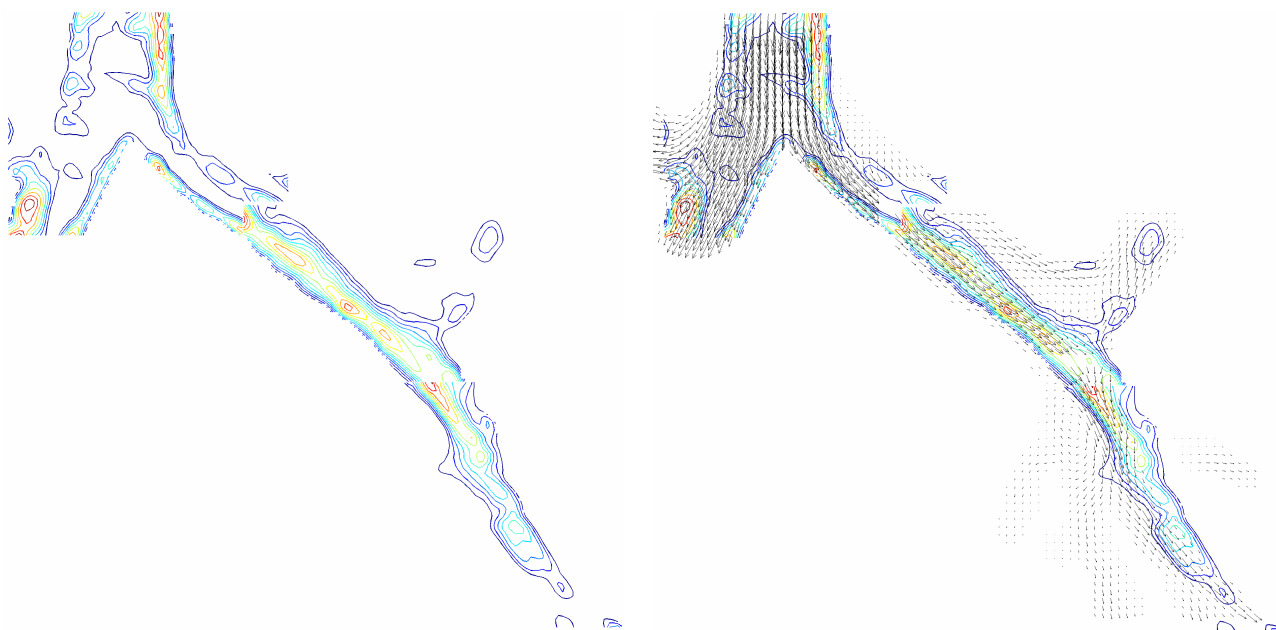


**Fig. 5** relative standard deviation of the velocity for stationary flow conditions at peak inspiration with  $Re = 1000$  (left), isolines of the standard deviation superposed to the velocity field (right)

## 4.2 Oscillatory flow

Figures 6a) and 6b) show exemplarily the results of the flow in the peak inspiration and peak expiration cycle for pulsating flow conditions. Since the Reynolds-number was defined with the mean bulk velocity at peak flow conditions it is again 1000 for the results shown below. The Womersley number is 3.24 and represents breathing at rest conditions.

A first comparison of the results for the inspiration and expiration phase demonstrates the different nature of the flow. During inspiration one can see larger flow separation regions at the outer walls of the bifurcating channels which sometimes even extend into the next bifurcation (Caro et al. 2002). In contrast, the flow at expiration does not separate at all and shows the typical jet-like profile in the center at the exit of the trachea. The overall values of shear are significantly lower than in the inspiration cycle. The complete cycle of inspiration and expiration suggests that due to the transformation of the velocity profiles and the generated separation regions a steady net mass

flow of fresh air is created into the model along the centerline and the inner walls of the bifurcations. This is compensated with a net mass outflow of used air to the trachea along the outer walls of the branches along the separation regions which are washed upstream during expiration. This effect called “steady streaming” was first mentioned by Haselton & Scherer (1982) and provides a net mass exchange in the pulsating lung flow. At higher breathing frequencies this effect is enhanced which may help to remove deposited particles in the lung network.

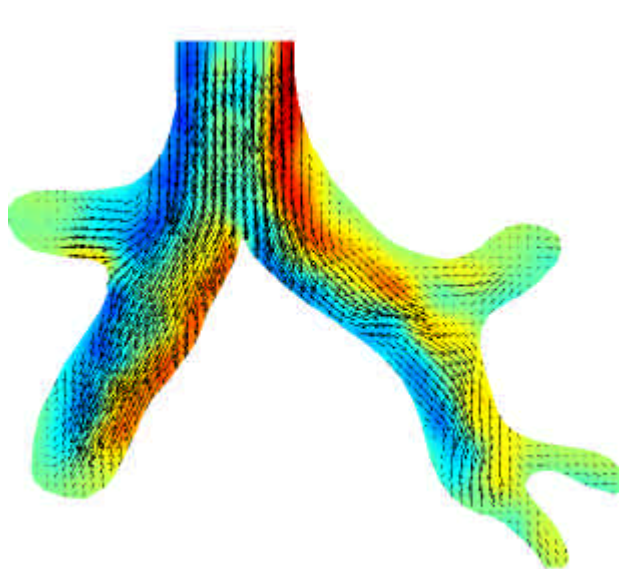


**Fig. 6a** Peak inspiration flow

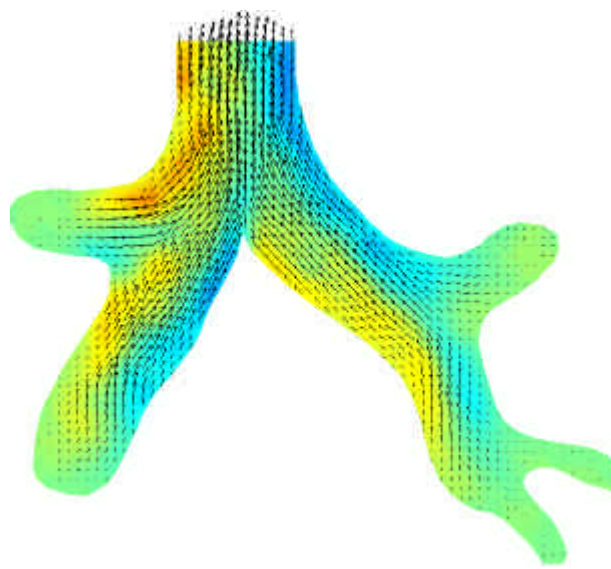


**Fig. 6b** Peak expiration flow

Figures 7a) till 8b) show the velocity profiles for peak - in- and outflow conditions. The Reynolds-number is again  $Re = 1000$  and the Womersley-number is 3.24 for the flow shown in figure 7a) and 7b) and 4.77 for the flow in figure 8a) and 8b).

According to Uchida (1956), the velocity profile changes from the parabolic shape to a two-peak shape at a Womersley - number of  $Wo = 3$ . This slightly annular shaped profile can also be seen in the trachea for all figures shown below. However, there is no significant difference between the profiles for  $Wo = 3.24$  and  $Wo = 4.77$ . The most distinctive annular shape exists for the profile in the carinal region. The location of the peak velocity is preserved in the daughter branches (Fig. 7a) and 8a) ) and the 2 - peak shaped profile vanishes. The profiles further downstream change to the 1-peak shape since the Womersley-number decreased due to the smaller diameter in the daughter branches. The velocity maximum is not located in the center of the tube but shifted towards the inner wall. This location represents again the mean flow direction as already stated above for the stationary flow.

A comparison of the velocity magnitude for in- and outflow shows a higher velocity for the inflow as can be seen at the vector lengths. It is similar for all flow conditions but the reference vector for the inflow is shorter.

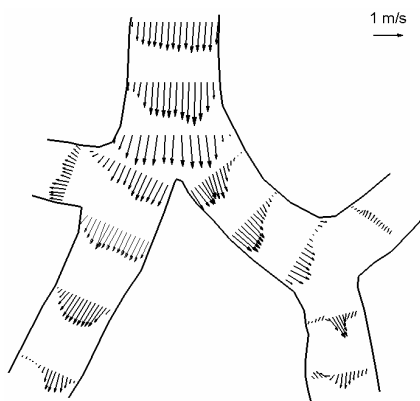


Fig. 7 a Maximum inspiration,  $Re = 1000$ ,  $Wo = 3.24$

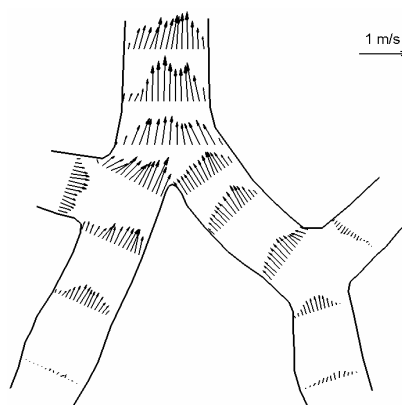


Fig. 7 b Maximum expiration,  $Re = 1000$ ,  $Wo = 3.24$

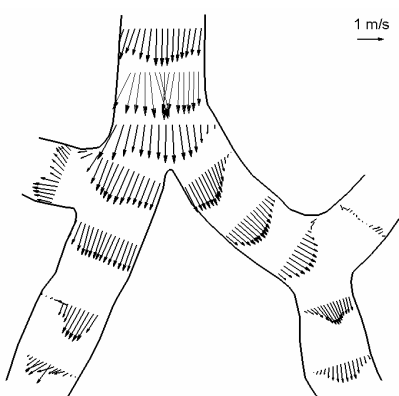


Fig. 8 a Maximum inspiration,  $Re = 1000$ ,  $Wo = 4.77$

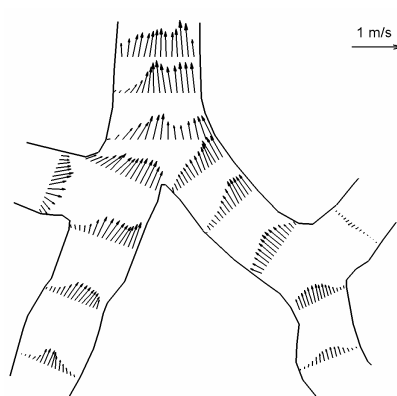


Fig. 8 b Maximum inspiration,  $Re = 1000$ ,  $Wo = 4.77$

#### 4. Summary and outlook

The flow characteristics for stationary and oscillating flow conditions through a model of the upper airways of the human lung have been analyzed using DPIV measurements. The stationary flow suggested a preferred flow direction through the network. However the flow passing the generations strongly varies with time as the calculation of the fluctuations could show.

The results for the oscillating flow demonstrate that there is a net mass flow of air into the lung along the inner walls and at the same time an outflow along the outer walls. This effect, called steady streaming, could herein be confirmed for a realistic lung model. The analysis of the velocity profiles showed that their shape is not preserved within one generation due to secondary flow effects flow separation. However the location of the velocity maximum remains constant in the transition region between the parent and the daughter branch for the inspiration and also from the daughter to the parent branch for the expiration.

A difference of the flow structure for the Womersley numbers of 3.24 and 4.77 could not be found. Further investigations need to be done with a wider range of Womersley- and also peak Reynolds-numbers. High frequency ventilation has to be investigated more in detail. Future studies will also incorporate a ventilation assist device connected to the trachea in order to investigate the flow interaction in the upper airways under such conditions typical for clinical respiratory treatment.

## Acknowledgements

This study was supported by DFG in the priority program: protective ventilation strategies, grant # BR 1494/7-1.

## References

- Brücker, Ch., Schröder, W. (2003) "Flow visualization in a model of the bronchial tree in the human lung airways via 3-D PIV", Proceedings of PSFVIP-4, June 3-5, Chamonix, France
- Fredberg J.J., Keefe D.H., Glass G.M., Castile R.G., Frantz I.D. (1984) "Alveolar pressure nonhomogeneity during smallamplitude high-frequency oscillation", *J. Appl. Physiol.* 57(3):788-800
- Haselton, F.R., Scherer, P.W. (1982) "Flow visualization of steady streaming in oscillatory flow through a bifurcating tube", *J. Fluid Mech.*, 123, 315-333
- Horsfield K, Cumming G. (1968) „Morphology of the bronchial tree in man”, *J Appl Physiol*; 24(3):373–383
- Horsfield K, Dart G. Olsen D.E. Filley G.F., Cumming G. (1971) „Models of the human bronchial tree”, *J Appl Physiol*; 31(2):207–217
- Marraro G. (1992) "Simultaneous independent lung ventilation in pediatric patients", *Crit Care Clin* 8, 131-145
- Mochizuki S. (2003) "Convective mass transport during ventilation in a model of branched airways of human lungs", Proceedings of PSFVIP-4, June 3-5, Chamonix, France
- Rettwitz-Volk W., Schlosser R. (1993) "One-sided high-frequency oscillating ventilation in the treatment of neonatal unilateral pulmonary emphysema"
- Tremblay L.N., Slutsky A.S (1998) "Ventilator-Induced Injury: From Barotrauma to Biotrauma", *Proceed Ass Am Physicians* 110: 482-488
- Uchida, S. (1956) "The Pulsating Viscous Flow Superposed on the Steady Laminar Motion of incompressible Fluid in a circular pipe", *ZAMP.*, Vol. VII
- Ultman J.S., Shaw R.G., Fabiano DC., Cooke K.A. (1988) "Pendelluft and mixing in a single bifurcation lung model during high-frequency oscillation", *J. Appl Physiol.* Jul; 65(1): 146-55
- Weibel, E.R. (1963) "Morphometry of the Human Lung", Springer, Berlin